Pion propagation at finite temperature

A. Schenk
Institute for Theoretical Physics, University of Bern, Sidlerstrasse 5, CH-3012 Bern, Switzerland
(Received 11 December 1992)

We calculate the pole shift of the pion up to second order in the density, considering the low-temperature expansion of the axial two-point function. To this order both absorptive and dispersive properties of pions are completely determined by two- and three-particle S-matrix elements. In particular, we show how the pole shift can be expressed in terms of these scattering amplitudes and discuss the size of corrections from three-particle collisions.

PACS number(s): 12.38.Mh, 11.30.Rd, 14.40.Aq, 25.75.+r

I. INTRODUCTION

It is common belief now that hadronic matter undergoes a deconfinement phase transition into a quark gluon plasma when the temperature reaches some critical value T_C [1]. Studying this expected phase transition is one of the main goals of experiments with high-energy nuclear collisions which in turn call for an improved theoretical understanding of the thermalization process occurring in the aftermath of such reactions. In particular, it is of interest to analyze absorptive and dispersive properties of hadrons below the critical temperature T_C.

In the present paper we analyze the propagation of pions through matter in a state of thermal equilibrium at temperature T. If the temperature is not too high the hadronic phase mainly consists of pions, the lightest particle of the theory, with effects of other massive excitations such as K, ρ, η, . . . being exponentially suppressed. At a temperature of 120 MeV every third particle is an excited state [2]. Although physics of the hadronic phase below the chiral phase transition has extensively been studied, most of the work is restricted to corrections of first order in the density. At this order the propagation of pions is described by a sequence of scattering processes involving only one particle of the heat bath at a time. If the temperature is not too high effects of the interaction with heavier excitations can be neglected and the corresponding shift in the pion pole is determined by the pion density and the $\pi\pi$ forward-scattering amplitude. The resulting corrections to absorptive and dispersive properties have been evaluated in two different ways: (i) by means of systematic low-temperature expansions in the framework of chiral perturbation theory [3–5] and (ii) in more realistic approaches [6,7] exploiting experimental information on $\pi\pi$ scattering amplitudes.

In the present paper we carry the expansion one step further and determine the pole shift of the pion up to second order in the density, including effects generated by three-body collisions. Absorptive and dispersive properties of pions in the heat bath are governed by the pion pole of the axial two-point function. We will make use of the fact that at low temperatures the low-energy properties of pions are controlled by chiral symmetry. Then the propagation properties can be analyzed in terms of an expansion which treats the temperature, the energy and the mass of the particles as small quantities (chiral perturbation theory). The leading term in this expansion describes the propagation of free particles with a pole at $\omega^2=\mathbf{p}^2+M_\pi^2$. The leading corrections to the pole shift are determined by the Bose factor and the current-algebra prediction for the $\pi\pi$ forward-scattering amplitude. To include effects of second order in the density we have to evaluate corrections one step beyond leading order in the low-temperature expansion. At this level, the contribution of first order in the density will involve the one-loop result for the $\pi\pi$ forward-scattering amplitude. Comparing this prediction with the results of an earlier work [6] which is based on a phenomenological description of this S-matrix element, we can provide a rather accurate estimate for the range of validity of chiral perturbation theory.

At second order in the density, the sequence of scattering processes the traversing pion undergoes will also involve events of simultaneous interaction with two particles of the heat bath at a time. In a second part of this paper we will furthermore show that the pole shift at this order in the density can still entirely be expressed in terms of S-matrix elements. The formula now involves both, two- and three-particle scattering amplitudes and provides an expression for the pole shift which should be valid even in ranges of temperature and momenta where chiral perturbation theory clearly breaks down. The discussion will also clarify the physical picture describing the propagation of particles in the heat bath, since effects of new phenomena such as the absence of asymptotic states in the medium clearly show up.

Perhaps we should also make a short remark about a technical point in this introduction. If the 2×2 matrix formulation of thermal field theory [8] is used, one generally encounters certain undefined quantities during finite temperature calculations, which some authors found difficult to deal with. We will show in this work that the occurrence of such terms is not inherent to finite temperature perturbation theory but the result of an untidy prescription which can be avoided.

II. REAL-TIME CHIRAL PERTURBATION THEORY

A very efficient technique for the analysis of the low-energy structure of the theory, in particular, for the

analysis of the low-temperature expansion, is provided by the effective Lagrangian method. Since this technique is described in detail in the literature for the case of zero temperature [10], we need only briefly discuss the extension to finite temperature [8,9], which is straightforward. In this framework pions are described by a field $U(x)$ which is defined on the group SU(2). The generating functional is represented as a path integral

$$e^{iZ[a_\mu,v_\mu,s,p]}=\int D\mu[U]\exp\left[i\int_C \mathcal{L}_{\rm eff}\,d^3x\,d\tau\right] . \tag{2.1}$$

The integration extends over all Euclidean space $\mathbb{R}^3$ and over a contour C in the complex time plane as shown in Fig. 1. The functional integral extends over field configurations with the periodicity condition

$$U(-\infty,\mathbf{x})=U(-\infty-i\beta,\mathbf{x}) ,$$

where $\beta=1/T$ is the inverse temperature.

$\mathcal{L}_{\rm eff}=\mathcal{L}_{\rm eff}(U,\nabla_\mu U,\nabla_\mu\nabla_\nu U,s,p,\ldots)$ is the standard effective Lagrangian [10] but the domain of definition for all fields is now the contour C instead of the real-time axis. Derivatives with respect to the complex time are taken along this contour. s and p are the external scalar and pseudoscalar densities. The external vector and axial-vector currents a_μ and v_μ are coupled to the field $U(x)$ by the covariant derivative

$$\nabla_\mu U=\partial_\mu U-i(v_\mu+a_\mu)U+iU(v_\mu-a_\mu) . \tag{2.2}$$

$\mathcal{L}_{\rm eff}$ is a sum of terms with an increasing number of derivatives and mass factors, corresponding to an expansion in powers of the momentum:

$$\mathcal{L}_{\rm eff}=\mathcal{L}^{(2)}+\mathcal{L}^{(4)}+\mathcal{L}^{(6)}+\cdots . \tag{2.3}$$

The leading term in this expansion is the well-known Lagrangian of the nonlinear σ model:

$$\mathcal{L}^{(2)}=\frac{F_0^2}{4}\langle\nabla_\mu U^\dagger\nabla^\mu U+M_0^2(U+U^\dagger)\rangle , \tag{2.4}$$

where angular brackets denote the trace in isospace. Since we are only interested in the axial-vector current, all other external sources are already switched off. F_0 is the pion decay constant in the chiral limit, i.e., $m_u=m_d=0$, while all other masses $(m_s,m_c,\ldots)$ are kept at their physical values. M_0 is the pion mass at leading order:

$$M_0^2=B_0(m_u+m_d) . \tag{2.5}$$

In our analysis isospin-breaking effects play only a minor role. Indeed, they do not show up at leading order because $\mathcal{L}^{(2)}$ is isospin invariant. The isospin breaking part of $\mathcal{L}^{(4)}$, being of order $(m_u-m_d)^2$, only shifts the mass of the π^0. But isospin breaking effects on the mass splitting are tiny, even as compared to electromagnetic contributions, and we therefore neglect them. Furthermore, we neglect all terms in $\mathcal{L}^{(4)}$ that do not contribute to the pole position. The remaining part of $\mathcal{L}^{(4)}$ involves four new low-energy constants L_1,L_2,L_4,L_6:

$$\begin{aligned}\mathcal{L}^{(4)}=&L_1\langle\nabla_\mu U^\dagger\nabla^\mu U\rangle^2+L_2\langle\nabla_\mu U^\dagger\nabla_\nu U\rangle\langle\nabla^\mu U^\dagger\nabla^\nu U\rangle\\&+L_4M_0^2\langle U^\dagger+U\rangle\langle\nabla_\mu U^\dagger\nabla^\mu U\rangle\\&+L_6M_0^4\langle U^\dagger+U\rangle^2 .\end{aligned} \tag{2.6}$$

For the full Lagrangian, including terms that are not relevant here, we again refer to the literature [10]. To determine the pole position at two-loop level, contributions from $\mathcal{L}^{(6)}$ enter only at the tree level. Since they are temperature independent and merely renormalize the pion mass, we need not consider them at all.

The low-temperature expansion of the effective functional $Z[a_\mu,v_\mu,s,p]$ is obtained by expanding the field $U(x)=e^{i\varphi\cdot\tau/F_0}$ in powers of φ^i. The leading term in the effective action is a quadratic form in φ^i which describes free mesons. The rest of the action is treated as a perturbation. Evaluating the Gaussian integrals in the standard manner one obtains a set of Feynman rules that differ from chiral perturbation theory at zero temperature only in one respect: All time integrations are replaced by integrations over the contour C and the propagator is the Green's function on this contour:

$$(\Box+M_0^2)\Delta_\beta(\tau-\tau',\mathbf{x}-\mathbf{x}')=-\delta_C(\tau-\tau')\delta^3(\mathbf{x}-\mathbf{x}') \tag{2.7}$$

with the solution

$$\begin{aligned}\Delta_\beta(\tau-\tau',\omega_p^0)=&-\frac{i}{2\omega_p^0}\frac{1}{1-e^{-\beta\omega_p^0}}\\&\times\{(e^{-i\omega_p^0(\tau-\tau')}+e^{-\beta\omega_p^0+i\omega_p^0(\tau-\tau')})\Theta_C(\tau-\tau')+(e^{i\omega_p^0(\tau-\tau')}+e^{-\beta\omega_p^0-i\omega_p^0(\tau-\tau')})\Theta_C(\tau'-\tau)\} ,\end{aligned} \tag{2.8}$$

which obeys Kubo-Martin-Schwinger boundary conditions. We use the notation $\Theta_C(\tau-\tau')$ and $\delta_C(\tau-\tau')$ for the θ and δ function, respectively, on the contour. In the following, real-time coordinates t will be represented by the symbols t^+ and t^-, depending on whether t belongs to the subset C^+ or the subset C^- of the contour C (see Fig. 1). In this language any time t_1^+ is later than any time t_2^-. The thermal propagator (2.8) contains a certain number of Green's functions, some of which will be used later in this work. From Eq. (2.8) we read off

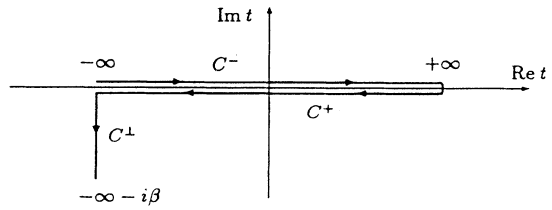

FIG. 1. The contour $C=C^-\cup C^+\cup C^\perp$ in the complex time plane runs from $t=-\infty$ along the real axis to $t=+\infty$, then back to $t=-\infty$ and from there down to $t=-\infty-i\beta$. The three portions are labeled C^-, C^+, and $C^\perp$.

$$i\Delta_\beta^{--}(z_1-z_2)\doteq i\Delta_\beta(t_1^- - t_2^-,\mathbf{z}_1-\mathbf{z}_2)$$
$$=\int\frac{d^dp}{(2\pi)^d}e^{-ip\cdot(z_1-z_2)}\frac{i}{p^2-M_0^2+i\epsilon}$$
$$+\vartheta(z_1-z_2)\,, \tag{2.9}$$
$$i\Delta_\beta^{-+}(z_1-z_2)\doteq i\Delta_\beta(t_1^- - t_2^+,\mathbf{z}_1-\mathbf{z}_2)$$
$$=\int\frac{d^dp}{(2\pi)^d}e^{-ip\cdot(z_1-z_2)}2\pi\delta(p^2-M_0^2)$$
$$\times\Theta(-p_0)+\vartheta(z_1-z_2)\,. \tag{2.10}$$

The temperature insertion

$$\vartheta(z_1-z_2)=\int\frac{d^dp}{(2\pi)^d}e^{-ip\cdot(z_1-z_2)}2\pi\delta(p^2-M_0^2)n_B(\omega_p^0)\,, \tag{2.11}$$

vanishes if the temperature is zero;

$$n_B(x)=\frac{1}{e^{\beta x}-1} \tag{2.12}$$

is the Bose distribution. Similar expressions can be derived for the functions Δ_β^{++} and Δ_β^{+-}. The retarded propagator

$$\Delta_R(z)=\int\frac{d^dp}{(2\pi)^d}e^{-ip\cdot z}\frac{1}{(p_0+i\epsilon)^2-(\omega_p^0)^2} \tag{2.13}$$

can then be expressed in terms of these functions as

$$\Delta_R=\Delta_\beta^{--}-\Delta_\beta^{-+}=\Delta_\beta^{+-}-\Delta_\beta^{++}\,. \tag{2.14}$$

Furthermore, at finite temperature, time ordering is replaced by ordering along the contour C, and the expectation value of the path-ordered two-point function of the axial-vector current is given by

$$i\langle T_C(A_{v_1}^{k_1}A_{v_2}^{k_2})\rangle=\frac{\delta}{\delta a_{v_1}^{k_1}}\frac{\delta}{\delta a_{v_2}^{k_2}}Z[a_\mu,v_\mu,s,p]\Big|_{\substack{v_\mu=a_\mu=p=0\\ s=M_0^2}}. \tag{2.15}$$

As for the propagator, we obtain, for the corresponding retarded function,

$$\langle R[A_{v_1}^{k_1}(t_1)A_{v_2}^{k_2}(t_2)]\rangle$$
$$\doteq\Theta(t_1-t_2)\langle[A_{v_1}^{k_1}(t_1),A_{v_2}^{k_2}(t_2)]\rangle$$
$$=\langle T_C[A_{v_1}^{k_1}(t_1^-)A_{v_2}^{k_2}(t_2^-)]\rangle$$
$$-\langle T_C[A_{v_1}^{k_1}(t_1^-)A_{v_2}^{k_2}(t_2^+)]\rangle\,. \tag{2.16}$$

Note that, on the subset C^- of the contour C, path ordering reduces to ordinary time ordering.

In the following we will use dimensional regularization because the Jacobian relating the measure $D\mu[U]$ to the measure $D\mu[\varphi]$ is equal to one in this scheme.

III. POLE SHIFT TO SECOND ORDER IN THE DENSITY

At tree level the path-ordered two-point function of the axial-vector current is just

$$i\langle T_C[A_{v_1}^{k_1}(z_1)A_{v_2}^{k_2}(z_2)]\rangle=\delta^{k_1k_2}F_0^2\Delta_{\beta v_1v_2}(z_1-z_2)$$
$$+\text{contact terms}\,, \tag{3.1}$$

where

$$\Delta_{\beta v_1v_2}(z_1-z_2)=\partial_{v_1}\partial_{v_2}\Delta_\beta(z_1-z_2)$$

is the second derivative of the thermal propagator (2.8) and the time derivatives are taken along the contour C. Applying Eqs. (2.14) and (2.16), the retarded two-point function is then

$$i\langle R[A_{v_1}^{k_1}(z_1)A_{v_2}^{k_2}(z_2)]\rangle=\delta^{k_1k_2}F_0^2\Delta_{Rv_1v_2}(z_1-z_2)$$
$$+\text{contact terms} \tag{3.2}$$

with the retarded propagator (2.13). Throughout this work we will neglect all contact terms without further mentioning it because they do not contribute to the pole position.

A. One-loop contribution

The relevant one-loop diagrams are summarized in Fig. 2. Straight lines represent the thermal propagator while the axial-vector current is indicated by the wiggly line. Vertices from the Lagrangians $\mathcal{L}^{(2)}$ and $\mathcal{L}^{(4)}$ are denoted by dots and filled squares, respectively.

The contributions of diagrams 2(a) and 2(b) are

$$F_0^2\delta^{k_1k_2}\int_C d^dx\,\Delta_{\beta v_1}(z_1-x)\Delta_{\beta v_2}(x-z_2)$$
$$\times\frac{M_0^2}{F_0^2}\left[\frac{i}{2}\Delta_\beta(0)+32\left[L_6-\frac{1}{2}L_4\right]M_0^2\right]$$
$$+\delta^{k_1k_2}\Delta_{\beta v_1v_2}(z_1-z_2)\left[\frac{2}{3}i\Delta_\beta(0)-16L_4M_0^2\right] \tag{3.3}$$

and from diagrams 2(c) and 2(d) we get

$$-\delta^{k_1k_2}\left[\frac{8}{3}i\Delta_\beta(0)-32L_4M_0^2\right]\Delta_{\beta v_1v_2}(z_1-z_2)\,. \tag{3.4}$$

To obtain these results we have performed partial integrations and made use of the following property of the

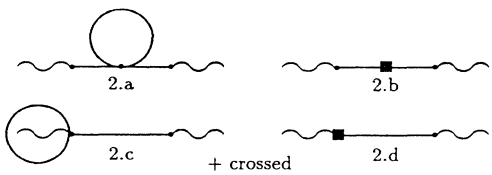

FIG. 2. One-loop contributions to the axial two-point function. Dots and filled squares indicate vertices from $\mathcal{L}^{(2)}$ and from $\mathcal{L}^{(4)}$. Wiggly lines represent axial-vector currents while full lines denote thermal propagators (2.8).

thermal propagator in the dimensional regularization scheme

$$\Box\Delta_\beta(0)=-M_0^2\Delta_\beta(0)\ . \tag{3.5}$$

Furthermore, although Lorentz invariance is lost at finite temperature, the first derivative of the thermal propagator still vanishes at the origin of space-time

$$\Delta_{\beta\nu}(0)=0\ . \tag{3.6}$$

Applying Eqs. (2.14) and (2.16) again, the Fourier transform of the axial two-point function is of the form

$$-\delta^{k_1k_2}F_0^2\,p_{\nu_1}p_{\nu_2}\Delta_R(p)[1+\delta f_1+\delta m_1^2\Delta_R(p)] \tag{3.7}$$

with

$$\delta f_1=\frac{M_0^2}{F_0^2}[16L_4-2i\Delta_\beta(0)M_0^{-2}]\ , \tag{3.8}$$

$$\delta m_1^2=\frac{M_0^4}{F_0^2}\left[32\left[L_6-\frac{1}{2}L_4\right]+\frac{i}{2}\Delta_\beta(0)M_0^{-2}\right]\ . \tag{3.9}$$

B. Two-loop contribution

So far we have considered contributions to both the residue and the pole position of the axial two-point function. To determine the pole shift at the two-loop level, it is, however, sufficient to know the residue at order F_0^{-2}. Thus, we can furthermore neglect all contributions to the residue from the two-loop diagrams.

The relevant two-loop graphs are summarized in Fig. 3. Let us first consider the momentum-dependent contributions. From diagram 3(a) we get

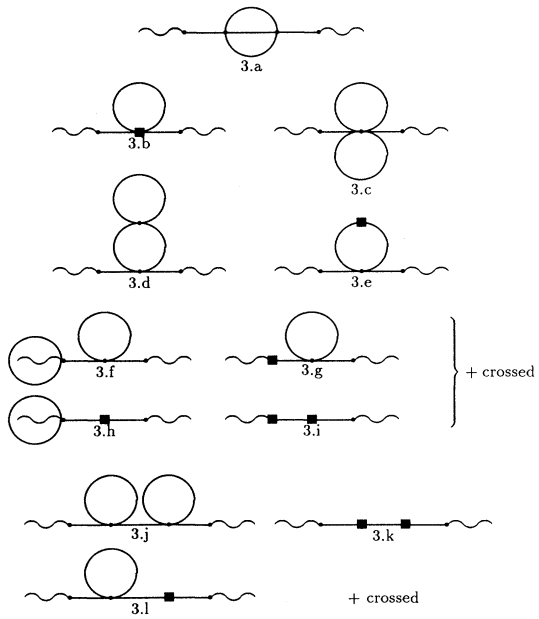

FIG. 3. Two-loop contributions to the pole shift of the axial two-point function. Dots and filled squares indicate vertices from $\mathcal{L}^{(2)}$ and from $\mathcal{L}^{(4)}$. Wiggly lines represent axial-vector currents while full lines denote thermal propagators (2.8).

$$\begin{aligned}-\delta^{k_1k_2}\frac{2}{3}\frac{1}{F_0^2}\int_C d^dx\,d^dy[&\Delta_\beta(y-x)\Delta_\beta^{\mu\nu}(y-x)-\Delta_\beta^{\mu}(y-x)\Delta_\beta^{\nu}(y-x)]\\ &\times[\Delta_{\beta\nu_1}(z_1-y)\Delta_{\beta\mu\nu}(y-x)\Delta_{\beta\nu_2}(x-z_2)+\Delta_{\beta\nu_1\nu}(z_1-y)\Delta_{\beta\mu}(y-x)\Delta_{\beta\nu_2}(x-z_2)\\ &+\Delta_{\beta\nu_1}(z_1-y)\Delta_{\beta\nu}(y-x)\Delta_{\beta\nu_2\mu}(x-z_2)+\Delta_{\beta\nu_1\nu}(z_1-y)\Delta_{\beta}(y-x)\Delta_{\beta\nu_2\mu}(x-z_2)]\\ &-\delta^{k_1k_2}\frac{5}{18}\frac{M_0^4}{F_0^2}\int_C d^dx\,d^dy\,\Delta_{\beta\nu_1}(z_1-y)\Delta_\beta^3(y-x)\Delta_{\beta\nu_2}(x-z_2)\ .\end{aligned} \tag{3.10}$$

Again the corresponding contribution to the retarded function is obtained in the standard manner, applying Eqs. (2.14) and (2.16) and using the propagators given in Eqs. (2.9) and (2.10). For the Fourier transform of this function we get so far

$$\begin{aligned}F_0^2\delta^{k_1k_2}p_{\nu_1}p_{\nu_2}\Delta_R^2(p)\int\frac{d^dq_1}{(2\pi)^d}\frac{d^dq_2}{(2\pi)^d}\frac{d^dq_3}{(2\pi)^d}(2\pi)^d\delta^{(d)}(p+q_1+q_2+q_3)F(p,q_1,q_2)\\ \times\frac{1}{6}[\Delta_\beta^{--}(q_1)\Delta_\beta^{--}(q_2)\Delta_\beta^{--}(q_3)-\Delta_\beta^{+-}(q_1)\Delta_\beta^{+-}(q_2)\Delta_\beta^{+-}(q_3)]\end{aligned} \tag{3.11}$$

with

$$F(p_1,p_2,p_3)=\frac{2}{3F_0^4}\left[\frac{5}{2}M_0^4+[(p_2-p_1)(p_4-p_3)]^2+[(p_3-p_1)(p_4-p_2)]^2+[(p_4-p_1)(p_3-p_2)]^2\right] \tag{3.12}$$

and p_4 being fixed by energy-momentum conservation.

From diagram 3(b) we obtain the following contribution to the pole term of the two-point function:

$$-F_0^2\delta^{k_1k_2}\int_C d^dx\,\Delta_{\beta\nu_1}(z_1-x)\Delta_{\beta\nu_2}(x-z_2)i\Delta_\beta(0)16\frac{M_0^4}{F_0^4}\left[3L_1+L_2+\frac{20}{3}L_6-\frac{13}{3}L_4\right]$$

$$-F_0^2\delta^{k_1k_2}\int_C d^dx\,\Delta^\mu_{\beta\nu_1}(z_1-x)\Delta^\nu_{\beta\nu_2}(x-z_2)\frac{32}{F_0^4}[i\Delta_{\beta\mu\nu}(0)(L_1+2L_2)]\ . \quad (3.13)$$

The second derivative of the thermal propagator at the origin of space-time can be written in a form which explicitly shows that Lorentz invariance is lost at finite temperature:

$$\Delta_{\beta\mu\nu}(0)=\frac{1}{d-1}[M_0^2\Delta_\beta(0)(-g_{\mu\nu}+n_\mu n_\nu)+\Delta_{\beta 00}(0)(-g_{\mu\nu}+dn_\mu n_\nu)]\ , \quad (3.14)$$

where $n_\mu=(1,\mathbf{0})$ is a constant four-vector. The second term in this equation involves the second derivative of the thermal propagator with respect to time. In this case the absence of Lorentz invariance is responsible for the fact that the contribution from diagram 3(b) to the self-energy is momentum dependent—at zero temperature it would only be a constant. The temperature-dependent part can be expressed in the form

$$F_0^2\delta^{k_1k_2}p_{\nu_1}p_{\nu_2}\Delta_R^2(p)\left[16\frac{M_0^4}{F_0^4}\left[3L_1+L_2+\frac{20}{3}L_6-\frac{13}{3}L_4\right]\vartheta(0)\right.$$

$$\left.+\frac{32}{F_0^4}(L_1+2L_2)\int\frac{d^dq}{(2\pi)^d}2\pi\delta(q^2-M_0^2)n_B(\omega_q^0)\frac{1}{4}(k^2-2M_0^2)^2\right]\ , \quad (3.15)$$

where $k=(p+q)$. Again we have omitted terms that merely renormalize the residue. All the remaining contributions to the self-energy depend only on temperature. From diagram 3(c) we readily get

$$F_0^2\delta^{k_1k_2}\int_C d^dx\,\Delta_{\beta\nu_1}(z_1-x)\Delta_{\beta\nu_2}(x-z_2)\left[\frac{25}{24}\frac{M_0^2}{F_0^4}\Delta_\beta^2(0)\right]\ . \quad (3.16)$$

From graphs 3(d) and 3(e) we obtain

$$F_0^2\delta^{k_1k_2}\int_C d^dx\,\Delta_{\beta\nu_1}(z_1-x)\Delta_{\beta\nu_2}(x-z_2)\left\{\frac{2}{3}\frac{M_0^2}{F_0^4}i\Delta_\beta(0)\left[i\Delta_\beta(0)+32\left[L_6-\frac{7}{8}L_4\right]M_0^2\right]+\frac{i}{2}\frac{M_0^2}{F_0^2}\delta m_1^2\int_C d^dy\,\Delta_\beta^2(x-y)\right\}\ . \quad (3.17)$$

In this expression the last integral over the contour C can be expressed in terms of the derivative of the thermal propagator with respect to its mass,

$$\partial_{M_0^2}\Delta_\beta(x)=\int_C d^dy\,\Delta_\beta(x-y)\Delta_\beta(y)\ , \quad (3.18)$$

and we will see below that this contribution just renormalizes the mass of the thermal distribution function.

If the 2×2 matrix formalism of thermal field theory [8] is employed, one generally encounters certain undefined quantities such as squares of δ functions during intermediate steps of finite temperature calculations. Although these terms cancel each other in the end, this is not a very satisfactory situation. In our case all these undefined quantities would arise from the evaluation of the Feynman graphs corresponding to diagrams 3(d) and 3(e). An explicit calculation would show that these quantities are introduced by an inadequate splitting of the contour integral (3.18) into a sum of ill-defined terms, thus their occurrence is not inherent to finite temperature perturbation theory but originates in mathematical untidiness.

The remaining diagrams 3(f)–3(l) are straightforward to calculate. We get the contribution

$$F_0^2\delta^{k_1k_2}\int_C d^dx\,d^dy\,\Delta_{\beta\nu_1}(z_1-x)\Delta_\beta(x-y)\Delta_{\beta\nu_2}(y-z_2)(\delta m_1^2)^2$$

$$+F_0^2\delta^{k_1k_2}\int_C d^dx\,\Delta_{\beta\nu_1}(z_1-x)\Delta_{\beta\nu_2}(x-z_2)\delta m_1^2\delta f_1+F_0^2\delta^{k_1k_2}\int_C d^dx\,\Delta_{\beta\nu_1}(z_1-x)\Delta_{\beta\nu_2}(x-z_2)$$

$$\times\delta m_1^2\frac{M_0^2}{F_0^2}\left[\frac{2}{3}i\Delta_\beta(0)M_0^{-2}-16L_4\right]\ , \quad (3.19)$$

where we have used the abbreviations δm_1^2 and δf_1 from Eqs. (3.8) and (3.9) for the shifts of the pole and the residue at one-loop level. In this expression the trivial terms $\sim(\delta m_1^2)^2$ and $\sim\delta m_1^2\delta f_1$ do not directly add to the pole shift of the axial two-point function. Only the last term provides a nontrivial contribution to the pole position. That such a contribution arises at all is due to the derivative coupling in chiral perturbation theory. Evaluating the corresponding one-particle reducible diagrams for the self-energy in, e.g., $\lambda\varphi^4$ theory, one only obtains the first term in Eq. (3.19).

IV. RENORMALIZATION

Most of the singularities in the limit $d=4$ stem from the thermal propagator at the origin of space-time and its derivative with respect to the mass. In the dimensional regularization scheme, we obtain

$$i\Delta_\beta(0)=2M_0^2\lambda+\vartheta(0) \tag{4.1}$$

with the singular part

$$\lambda=\frac{1}{(4\pi)^2}\mu^{d-4}\left\{\frac{1}{d-4}-\frac{1}{2}\left[\Gamma'(1)+1+\ln(4\pi)-\ln\left[\frac{M_0^2}{\mu^2}\right]\right]\right\}. \tag{4.2}$$

The temperature-dependent part $\vartheta(0)$ is finite [see Eq. (2.11)]. For the derivative we get the similar expression

$$i\partial_{M_0^2}\Delta_\beta(0)=2\lambda+\frac{1}{(4\pi)^2}+\partial_{M_0^2}\vartheta(0)\ . \tag{4.3}$$

Again the temperature-dependent term is finite.

The singularity structure in Eq. (3.11) is more complicated. In the representation [Eqs. (2.9) and (2.10)] for the propagators $\Delta_\beta^\pm$ we have separated the temperature-dependent part ϑ from the limit of these propagators at $T=0$. Multiplying out the propagators in Eq. (3.11) we can identify three different contributions in this equation. The first one is the temperature-independent limit $T=0$. The other two are of first and second order in the Bose factor n_B, respectively. Furthermore, the contribution of first order develops a pole at the dimension $d=4$ while the second-order term is finite. Performing the loop integrations with respect to q_2 and q_3 we obtain, for the first-order term,

$$\int\frac{d^dq}{(2\pi)^d}2\pi\delta(q^2-M_0^2)n_B(\omega_q^0)\left[\frac{1}{3}\lambda\frac{1}{F_0^4}[10(k^2-2M_0^2)^2+13M_0^4]+\frac{1}{96\pi^2F_0^4}\left[\frac{28}{3}(k^2-2M_0^2)^2+\frac{23}{3}M_0^4\right]-\frac{5}{48\pi^2F_0^4}\bar{J}\left[\sigma(k^2)\right]\left[k^4-\frac{16}{5}k^2M_0^2+\frac{37}{10}M_0^4\right]\right] \tag{4.4}$$

with $k=(p+q)$ and

$$\bar{J}(\sigma)=2+\sigma\ln\left[\frac{\sigma-1}{\sigma+1}\right],\quad \sigma(x)=\left[1-\frac{4M_0^2}{x}\right]^{1/2}.$$

The bare coupling constants L_1, L_2, L_4, and L_6 all contain a pole at $d=4$. Let us define the renormalized coupling constants $\bar{L}_i$ by

$$L_i=\delta_i\lambda+\bar{L}_i \tag{4.5}$$

with

$$\delta_1=\tfrac{1}{12},\quad \delta_2=\tfrac{1}{6},\quad \delta_4=\tfrac{1}{4},\quad \delta_6=\tfrac{3}{32}. \tag{4.6}$$

With this definition all our results remain finite if the regularization is removed.

Indeed, the requirement for the one-loop results [Eqs. (3.8) and (3.9)] to be finite, uniquely fixes the constants δ_4 and δ_6, yielding

$$\delta f_1=\frac{M_0^2}{F_0^2}[16\bar{L}_4-2\vartheta(0)M_0^{-2}], \tag{4.7}$$

$$\delta m_1^2=\frac{M_0^4}{F_0^2}\left[32\left[\bar{L}_6-\frac{1}{2}\bar{L}_4\right]+\frac{1}{2}\vartheta(0)M_0^{-2}\right]. \tag{4.8}$$

The reader should be aware of the differences between the parameters F_0 and M_0 and their physical values F_π and M_π, which at this level of accuracy are given by the well known result

$$M_\pi^2=M_0^2\left[1+32\frac{M_0^2}{F_0^2}\left[\bar{L}_6-\frac{1}{2}\bar{L}_4\right]\right], \tag{4.9}$$

$$F_\pi^2=F_0^2\left[1+16\frac{M_0^2}{F_0^2}\bar{L}_4\right]. \tag{4.10}$$

These relations enable us to express the temperature dependence of the mass and the decay constant in terms of the physical quantities:

$$M_\pi^2(T)=M_\pi^2+\frac{1}{2}\frac{M_\pi^2}{F_\pi^2}\vartheta(0)\sim M_\pi^2\left[1+\frac{1}{2}\frac{M_\pi^2}{F_\pi^2}\left[\frac{T}{2\pi M_\pi}\right]^{3/2}e^{-M_\pi/T}\right], \tag{4.11}$$

$$F_\pi^2(T)=F_\pi^2-2\vartheta(0)\sim F_\pi^2\left[1-2\frac{M_\pi^2}{F_\pi^2}\left[\frac{T}{2\pi M_\pi}\right]^{3/2}e^{-M_\pi/T}\right]. \tag{4.12}$$

Furthermore, one readily obtains the following results in the chiral limit $M_0=0$:

$$M_\pi(T)=0\ ,\quad F_\pi^2(T)=F_\pi^2\left[1-\frac{1}{6}\left[\frac{T}{F_\pi}\right]^2\right]\ . \tag{4.13}$$

Actually, these one-loop results for the mass and the decay constant are not new [4] and may be considered as a check for our calculation. In accordance with unitarity we do not observe any absorption at leading order. Furthermore, dispersion is also absent: at the one-loop level interaction with the heat bath only modifies the mass and the decay constant which both become temperature dependent.

At the two-loop level we obtain the following expansion of the retarded two-point function of the axial-vector current in powers of F_0^{-2}:

$$\begin{aligned}&-\delta^{k_1k_2}F_0^2\,p_{\nu_1}p_{\nu_2}\Delta_R(p)\\&\quad\times\{1+\delta f_1+\delta f_2+\Delta_R(p)(\delta m_1^2+\delta m_1^2\delta f_1+\Sigma_2)\\&\qquad+[\delta m_1^2\Delta_R(p)]^2\}\ .\end{aligned} \tag{4.14}$$

The one-loop contributions δf_1 and δm_1^2 [see also Eq. (3.7)] are of order F_0^{-2} while δf_2 and Σ_2 are of order F_0^{-4}. The two-loop contribution δf_2 merely renormalizes the residue and has already been neglected. If we define the retarded self-energy Σ_R by

$$\Sigma_R(p^0,\mathbf{p})=M_0^2+\delta m_1^2+\Sigma_2(p^0,\mathbf{p})\ , \tag{4.15}$$

Eq. (4.14) is just the geometric series of the function

$$-\delta^{k_1k_2}p_{\nu_1}p_{\nu_2}\frac{F_0^2(1+\delta f_1+\delta f_2)}{(p_0+i\epsilon)^2-\mathbf{p}^2-\Sigma_R}\ . \tag{4.16}$$

As in the discussion of Eq. (4.4) we can in general divide this self-energy into three pieces:

$$\Sigma_R=\Sigma_R^{(0)}+\Sigma_R^{(1)}+\Sigma_R^{(2)}\ , \tag{4.17}$$

where $\Sigma_R^{(0)}$ is the zero-temperature result and $\Sigma_R^{(1)}$ and $\Sigma_R^{(2)}$ are the contributions of first and second order in the Bose factor n_B, respectively. The discussion in the previous section already showed that higher powers in the Bose factor do not occur at the two-loop level. In the following we will also use the abbreviation

$$\Sigma_R^T\doteq\Sigma_R^{(1)}+\Sigma_R^{(2)} \tag{4.18}$$

for the full temperature-dependent contribution. By definition this contribution vanishes if the temperature goes to zero.

The temperature-independent piece $\Sigma_R^{(0)}$ still has a pole at $d=4$. To remove this singularity we have to add further counterterm diagrams such as the one given in Fig. 2(b), but with the vertices from the Lagrangian $\mathcal{L}^{(6)}$. Together, we get an additional finite contribution of order M_0^4/F_0^4 to the physical value of the pion mass M_π, which is then given by

$$M_\pi^2=M_0^2\left[1+32\frac{M_0^2}{F_0^2}\left[\bar{L}_6-\frac{1}{2}\bar{L}_4\right]+\frac{M_0^4}{F_0^4}c\right]\ . \tag{4.19}$$

The momentum dependence of the term $\Sigma_R^{(0)}$ stems entirely from the two-loop diagrams and is of order F_0^{-4}; hence, it only affects the residue. If the self-energy is expressed in terms of the physical mass, the quantity $\Sigma_R^{(0)}$ can be eliminated and the pole position is determined by the equation

$$(p^0)^2=\mathbf{p}^2+M_\pi^2+\Sigma_R^T(p^0,\mathbf{p}). \tag{4.20}$$

In the limit $T=0$ the pole is indeed at the position $p^0=\sqrt{\mathbf{p}^2+M_\pi^2}$. At nonzero temperature and for real wave numbers the pole sits at a complex value of p^0:

$$p^0=\omega(p)-\frac{i}{2}\gamma(p)\ . \tag{4.21}$$

$\omega(p)$ is the frequency of pionic waves with wave number p and $M_\pi(T)\doteq\omega(p=0)$ is the effective mass. The damping coefficient $\gamma(p)$ is the inverse time within which the intensity of the wave is attenuated by a factor $1/e$. In leading order of small quantities, absorption and dispersion are given by

$$\omega(p)=\sqrt{\mathbf{p}^2+M_\pi^2+\mathrm{Re}\Sigma_R^T(\omega_p,\mathbf{p})} \tag{4.22}$$

$$\approx\omega_p+\frac{1}{2\omega_p}\,\mathrm{Re}\Sigma_R^T(\omega_p,\mathbf{p})\ , \tag{4.23}$$

$$\gamma(p)=-\frac{1}{\omega_p}\,\mathrm{Im}\Sigma_R^T(\omega_p,\mathbf{p})\ , \tag{4.24}$$

where $\omega_p\doteq\sqrt{\mathbf{p}^2+M_\pi^2}$ is the pole position in the limit $T=0$ and Σ_R^T describes the modification by the interaction with the heat bath.

At one-loop level this interaction modifies the pion mass which becomes a function of temperature. At next order, therefore, we expect terms accounting for the fact that the thermal distribution of these particles actually depends on their effective mass at temperature T instead of the bare quantity. From diagrams 3(d) and 3(e) we indeed get the next term in an expansion of the Bose factor around its bare mass M_0. Together with the one-loop result we obtain the contribution

$$\begin{aligned}&\frac{1}{2}\frac{M_0^2}{F_0^2}[\vartheta(0,M_0^2)+\delta m_1^2\partial_{M_0^2}\vartheta(0,M_0^2)]\\&\qquad=\frac{1}{2}\frac{M_0^2}{F_0^2}\vartheta(0,M_\pi^2(T))\ ,\end{aligned} \tag{4.25}$$

which involves corrections of second order in the density.

The requirement for the singularities of the first-order term $\Sigma_R^{(1)}$ to cancel each other uniquely fixes the remaining two constants δ_1 and δ_2 at the values given in Eq. (4.6). If the regularization is finally removed we obtain the results

$$\Sigma_R^{(1)}(\omega_p,\mathbf{p})=\vartheta(0,M_\pi^2)\left\{\frac{1}{2}\frac{M_0^2}{F_0^2}-\frac{M_0^4}{F_0^4}\left[64\left[\bar{L}_6-\frac{1}{2}\bar{L}_4\right]+80(\bar{L}_1+\bar{L}_2)-\frac{31}{64\pi^2}\right]\right\}$$
$$-\int\frac{d^3q}{(2\pi)^3 2\omega_q}n_B(\omega_q)\left[\frac{s(s-4M_0^2)}{F_0^4}\left[16(\bar{L}_1+2\bar{L}_2)-\frac{7}{36\pi^2}\right]+\frac{\bar{J}[\sigma(s)]}{96\pi^2F_0^4}(10s^2-32M_0^2s+37M_0^4)\right.$$
$$\left.+\frac{\bar{J}[\sigma(u)]}{96\pi^2F_0^4}(10u^2-32M_0^2u+37M_0^4)\right] \tag{4.26}$$

with the Mandelstam variables $s=(p+q)^2$ and $u=(p-q)^2$, and

$$\Sigma_R^{(2)}(\omega_p,\mathbf{p})=\frac{1}{2}\frac{M_0^2}{F_0^2}[\vartheta(0,M_\pi^2(T))-\vartheta(0,M_\pi^2)]-\frac{1}{24}\frac{M_0^2}{F_0^4}[\vartheta(0)]^2$$
$$+\tfrac{1}{2}\int\frac{d^4q_1}{(2\pi)^4}\frac{d^4q_2}{(2\pi)^4}\frac{d^4q_3}{(2\pi)^4}(2\pi)^4\delta^{(4)}(p+q_1+q_2+q_3)F(p,q_1,q_2)(2\pi)^2\delta(q_1^2-M_0^2)\delta(q_2^2-M_0^2)$$
$$\times n_B(\omega_{q_1}^0)n_B(\omega_{q_2}^0)\left[\frac{1}{q_3^2-M_0^2+i\epsilon}+2i\pi\delta(q_3^2-M_0^2)\Theta(q_3^0)\right] \tag{4.27}$$

with the function F given in Eq. (3.12). Furthermore, we separated contributions coming from Eq. (4.25) according to their order in the density.

The result for the self-energy confirms a general property of finite temperature perturbation theory. If the coupling constants are renormalized in such a way that the theory is finite in the limit $T=0$, then it remains finite if the temperature is switched on: additional singularities do not occur at nonzero temperature. Indeed, the numerical values for the constants δ_i in Eq. (4.6) agree with the one-loop calculation at zero temperature [10].

V. S-MATRIX ELEMENTS

The relevant $\pi\pi$ forward-scattering amplitude

$$T_{\pi\pi}(s)=\sum_{\pi'=\pi^0,\pi^\pm}T_{\pi\pi'}(s) \tag{5.1}$$

can be expressed in terms of the amplitude $A(s,t,u)$:

$$T_{\pi\pi}(s)=A(s,0,u)+3A(0,u,s)+A(u,s,0)\ . \tag{5.2}$$

At one-loop order this amplitude is given by [10]

$$A(s,t,u)=\frac{s-M_0^2}{F_0^2}+B(s,t,u)+C(s,t,u)\ ,$$
$$B(s,t,u)=\frac{1}{96\pi^2F_0^4}\{3(s^2-M_0^4)\bar{J}(s)+[t(t-u)-2M_0^2t+4M_0^2u-2M_0^4]\bar{J}(t)$$
$$+[u(u-t)-2M_0^2u+4M_0^2t-2M_0^4]\bar{J}(u)\}\ , \tag{5.3}$$
$$C(s,t,u)=\frac{1}{96\pi^2F_0^4}\left[8\left[96\pi^2\bar{L}_1-\frac{1}{3}\right](s-2M_0^2)^2+2\left[96\pi^2\bar{L}_2-\frac{5}{12}\right][s^2+(t-u)^2]-12M_0^2s+15M_0^4\right]\ .$$

In addition to the mass and the decay constant this equation additionally involves the four new low-energy constants $\bar{L}_1$, $\bar{L}_2$, $\bar{L}_4$, and $\bar{L}_6$, which are not fixed by chiral symmetry. To eliminate these parameters, further physical quantities have to be introduced. The parameters $\bar{L}_4$ and $\bar{L}_6$ enter these relations through the physical values of the pion mass and the decay constant. The numerical values of the low-energy constants can be estimated by a phenomenological analysis based on experimental information on $\pi\pi$ scattering at low energies. The behavior of the $\pi\pi$ partial-wave amplitudes near threshold is described by the $\pi\pi$ scattering lengths a_l^I and by the slope parameters b_l^I which depend on these four constants through Eq. (5.3). For the detailed discussion of this analysis we again refer the reader to the literature [10]. For the numerical computation discussed below we need to eliminate the bare quantities from Eq. (4.26) using the relations

$$\frac{32\pi}{3}(a_0^0+5a_0^2)=-\frac{M_0^2}{F_0^2}+32\frac{M_0^4}{F_0^4}\left[5(\bar{L}_1+\bar{L}_2)+4\left[\bar{L}_6-\frac{1}{2}\bar{L}_4\right]+\frac{15}{1024\pi^2}\right],$$

$$a_2^0=\frac{4}{15\pi F_0^4}\left[\bar{L}_1+2\bar{L}_2-\frac{53}{3072\pi^2}\right]. \tag{5.4}$$

From Eqs. (5.3) and (5.4) we readily obtain for the $\pi\pi$ forward-scattering amplitude

$$T_{\pi\pi}(s)=\frac{32\pi}{3}(a_0^0+5a_0^2)-\frac{23}{16\pi^2}\frac{M_\pi^4}{F_\pi^4}+s(s-4M_\pi^2)\left[60\pi a_2^0+\frac{47}{576\pi^2F_\pi^4}\right]+\frac{\bar{J}[\sigma(s)]}{96\pi^2F_\pi^4}(10s^2-32M_\pi^2s+37M_\pi^4)$$

$$+\frac{\bar{J}[\sigma(u)]}{96\pi^2F_\pi^4}(10u^2-32M_\pi^2u+37M_\pi^4). \tag{5.5}$$

The comparison with expression (4.26) shows that we can express the contribution of first order in the density to the pole shift in terms of this S-matrix element:

$$\Sigma_R^{(1)}=-\int\frac{d^3q}{(2\pi)^3 2\omega_q}n_B(\omega_q)T_{\pi\pi}(s). \tag{5.6}$$

In the rest of this section we will show how the contribution of second order in the density can be expressed in a similar way involving a three-particle forward-scattering amplitude. Because of the singular behavior of three-particle amplitudes in the physical region their forward limit can only be taken after some of the poles have been removed in a well-defined way. This leads to the definition of what we call proper three-particle scattering amplitude.

Let us be more precise and recall some well-known facts [11] about physical region poles of three-particle scattering amplitudes $T_{33}(p_1,p_2,p_3;p_4,p_5,p_6)$ with three ingoing momenta p_1,p_2,p_3 and three outgoing momenta p_4,p_5,p_6. For the sake of simplicity we restrict this discussion to spinless particles with mass M.

Unitarity requires that three-particle amplitudes in general contain contributions of the form

$$-T_{22}\frac{1}{q^2-M^2+i\epsilon}T_{22}, \tag{5.7}$$

where the four-momentum q is a cross-energy variable, e.g., $q=(p_1+p_2-p_4)$, and T_{22} is the two-particle scattering amplitude. (The two matrix elements in this equation describe processes with different ingoing and outgoing momenta.)

The physical interpretation of these infinities of an amplitude in the physical region has extensively been discussed in the literature [12] and can be summarized as follows: If we consider a general scattering experiment, the lines of flight of the particles are overwhelmingly likely to miss one another, or at most to interact in groups. This idea leads to the connectedness structure of S-matrix elements. The next most likely possibility is that first one set of particles interacts, and that at a later time one of the particles emerging from this interaction scatters with another set of these particles. The pole at $q^2=M^2$ occurring in Eq. (5.7) just expresses the fact that it is infinitely more likely for the particles to interact in two successive events than to interact simultaneously. Between these two processes the "intermediate" particle with four-momentum q is (nearly) on its mass shell and thus can propagate over large distances in space-time.

Some of the terms in Eq. (5.7), e.g., if $q=(p_1+p_2-p_6)$, do have a well-defined forward limit, defined by $p_i=p_{i+3}$, $(i=1,2,3)$, while for others, e.g., if $q=(p_1+p_2-p_4)$, this limit does not exist. In view of Eq. (5.7) we define the proper three-particle amplitude $\hat{T}_{33}$ to be

$$\hat{T}_{33}\doteq T_{33}+\sum_q{}'T_{22}\frac{1}{q^2-M^2+i\epsilon}T_{22}. \tag{5.8}$$

The prime indicates summation over all four-momenta that become singular in the forward limit, i.e., for which $q^2\to M^2$. Per construction this amplitude does have a well-defined forward limit.

S-matrix elements are, in general, well-defined quantities on the mass shell, whose off-shell extrapolations are not determined by any physical properties. The definition of the proper three-particle amplitude $\hat{T}_{33}$, on the other hand, does depend on the off-shell behavior of the two-particle S-matrix elements in Eq. (5.8). To remove the singularities it is sufficient to put all momenta in these amplitudes on the mass shell. But if we allow the momentum q to be off shell, we would also remove some part of the regular contributions and obtain a proper amplitude which depends on the off-shell extrapolation of the two-particle scattering element. Physically the question is how much of the three-particle S-matrix element should be ascribed to double scattering and which part really describes simultaneous three-particle interaction. Let us first discuss the consequences when all momenta are restricted to the mass shell. Later we will naturally be lead to include off-shell effects (see next section).

The physical content of the mathematical prescription in Eq. (5.8) is readily understood in the phenomenological language introduced above. For contributions with a well-defined forward limit the residue of the pole at

$q^2=M^2$ is the square of a two-particle scattering amplitude with nonvanishing momentum transfer, thus describing double scattering with momentum transfer in each event, while in the other cases it is a product of two different two-particle forward-scattering amplitudes. For the cross-energy variable $q=(p_1+p_2-p_6)$, for example, we get the forward limit $q=(p_1+p_2-p_3)$ and the residue $(T_{22})^2(p_1,p_2;p_3,q')$ with q' on the mass shell, while, for example, for $q=(p_1+p_2-p_4)$ we obtain the residue

$$T_{22}(p_1,p_2;p_1,p_2)T_{22}(p_3,p_2;p_3,p_2)\ .$$

Thus, to get the proper three-particle forward-scattering amplitude, one has to remove all those double-scattering contributions from the full S-matrix element, that involve two successive two-particle forward-scattering processes separated by large space-time distances. In fact, some of these contributions should already be included in Eq. (5.6), and one has to remove double forward-scattering processes also on physical grounds in order to avoid double counting. Indeed, cutting both loop lines in diagram 3(j) with a temperature insertion, one obtains a Feynman graph describing two successive forward-scattering events. This effect is completely accounted for by the first term in expression (3.19) and thus yields just the next-to-leading-order term in the geometric expansion (4.14).

We finish this general discussion with a last remark about unitarity, which requires the following relation for the imaginary part of the full three-particle scattering amplitude:

$$\mathrm{Im}T_{33}=2\pi\sum_q T_{22}\delta(q^2-M^2)T_{22}+\text{higher}\ , \tag{5.9}$$

where "higher" contributions involve S-matrix elements with more than two ingoing or outgoing particles. From Eq. (5.8) we immediately infer the same unitarity relation for the proper (forward-) scattering amplitude, but there the summation only extends over a proper subset of cross-energy variables q.

The relevant three-pion scattering amplitude

$$T_{\pi\pi\pi}\doteq\sum_{\pi',\pi''=\pi^{\pm},\pi^0}T_{\pi\pi'\pi'',\pi\pi'\pi''} \tag{5.10}$$

has the following form at tree level:

$$T_{\pi\pi\pi}=+\frac{25}{3}\frac{M_0^2}{F_0^4}+\frac{P_{123}}{(p_1+p_2+p_3)^2-M_0^2}+\frac{P_{124}}{(p_1+p_2-p_4)^2-M_0^2}+\cdots\ . \tag{5.11}$$

The sum extends over all cross-energy variables and the P_{ijk} are polynomials in the momenta of order p^4. The explicit form of this result is straightforward to calculate but quite lengthy; hence, we will only sketch the procedure described above. With the definition $p_i\doteq p_{i+3}+\epsilon_i$ $(i=1,2,3)$, the forward limit is taken by sending the ϵ's to zero. Let us consider the cross term with $q=p_1+p_2-p_4=p_2+\epsilon_1$ as an example and neglect contributions of order ϵ_1^2. Then we get for the corresponding polynomial

$$P_{124}=-\frac{M_0^2}{F_0^4}(M_0^2-2\epsilon_3^2)-\frac{8}{3}\frac{M_0^2-\epsilon_3^2}{F_0^4}p_2\cdot\epsilon_1+O(\epsilon_1^2) \tag{5.12}$$

and for the relevant product of the two-particle scattering amplitudes

$$\begin{aligned}\frac{1}{3}&T_{\alpha\beta\alpha\delta}(p_1,p_2;p_4,q)T_{\delta\gamma\beta\gamma}(q,p_3;p_5,p_6)\\&=T_{\pi\pi}(p_1,p_2;p_4,q)T_{\pi\pi}(q,p_3;p_5,p_6)\\&=\frac{1}{F_0^4}(M_0^2-2\epsilon_3^2)(M_0^2-2\epsilon_1^2)\ .\end{aligned} \tag{5.13}$$

Thus we get the contribution $-4M_0^2/(3F_0^4)$ from the regular term in Eq. (5.12) to the forward limit. Finally, we obtain the following result for the proper forward-scattering amplitude:

$$\begin{aligned}\hat{T}_{\pi\pi\pi}(p_1,p_2,p_3)=&\frac{1}{3}\frac{M_0^2}{F_0^4}-\frac{F(p_1,p_2,p_3)}{(p_1+p_2+p_3)^2-M_0^2}-\frac{F(p_1,p_2,-p_3)}{(p_1+p_2-p_3)^2-M_0^2}-\frac{F(p_1,-p_2,p_3)}{(p_1-p_2+p_3)^2-M_0^2}\\&-\frac{F(p_1,-p_2,-p_3)}{(p_1-p_2-p_3)^2-M_0^2}\ ,\end{aligned} \tag{5.14}$$

where the polynomial F is given in Eq. (3.12).

This result enables us to write the full self-energy Σ_R^T in the form

$$\begin{aligned}\Sigma_R^T(\omega_p,\mathbf{p})=&-\int\frac{d^3q}{(2\pi)^3 2\omega_q^T}n_B(\omega_q^T)T_{\pi\pi}(s)\\&-\frac{1}{2}\int\frac{d^3q_1}{(2\pi)^3 2\omega_{q_1}}\frac{d^3q_2}{(2\pi)^3 2\omega_{q_2}}n_B(\omega_{q_1})\\&\times n_B(\omega_{q_2})\hat{T}^R_{\pi\pi\pi}(p,q_1,q_2)\ ,\end{aligned} \tag{5.15}$$

where we have introduced the abbreviation $(\omega_p^T)^2\doteq\mathbf{p}^2+M_\pi^2(T)$ and the retarded function

$$\begin{aligned}\hat{T}^R_{\pi\pi\pi}(p_1,p_2,p_3)\doteq&\hat{T}_{\pi\pi\pi}(p_1,p_2,p_3)\\&-2\pi i\delta^{(+)}((p_2+p_3-p_1)^2-M_0^2)\\&\times F(p_1,-p_2,-p_3)\ .\end{aligned} \tag{5.16}$$

The three-particle S-matrix element (5.11) is the amputated time-ordered six-point function of the axial-vector current. The function in Eq. (5.16) is called retarded, because it is just (the proper forward limit of) the corre-

sponding amputated six-point function with retarded boundary conditions. The momentum p_1 is conjugate to the distinguished space-time variable $(t_1,\mathbf{x}_1)$ such that this retarded function is zero for any other time being later than t_1. We will comment on the occurrence of these boundary conditions below.

The representation (5.15) and the explicit expressions for the functions $T_{\pi\pi}$ and $\hat{T}^R_{\pi\pi\pi}$ given in Eqs. (5.5) and (5.16) constitute the main result of the present paper. It specifies the position of the pion pole as a function of temperature according to Eq. (4.20) and is valid up to and including contributions of order p^6 in the chiral expansion.

Unitarity relations for the two- and three-particle scattering amplitude allow us to rewrite the expression for the damping of pionic waves in the form

$$\gamma(p)=\frac{1}{4\omega_p}\frac{1}{1+n_B(\omega_p)}\int\frac{d^3q_1}{(2\pi)^3 2\omega_{q_1}}\frac{d^3q_2}{(2\pi)^3 2\omega_{q_2}}\frac{d^3q_3}{(2\pi)^3 2\omega_{q_3}}(2\pi)^4\delta^{(4)}(p+q_1+q_2+q_3)$$
$$\times n_B(\omega_{q_1})[1+n_B(\omega_{q_2})][1+n_B(\omega_{q_3})]|T_{\pi\pi}(s,t)|^2\ , \tag{5.17}$$

which explicitly shows that Bose correlation is accounted for in both, initial and final states. To obtain this result we used the exact identity

$$\frac{1}{1+n_B(\omega_1)}n_B(\omega_2)[1+n_B(\omega_3)][1+n_B(\omega_4)]$$
$$=n_B(\omega_2)+n_B(\omega_2)n_B(\omega_3)+n_B(\omega_2)n_B(\omega_4)$$
$$-n_B(\omega_3)n_B(\omega_4)\ , \tag{5.18}$$

which holds if energy is conserved. The representation (5.17) involves the isospin averaged S-matrix element $T_{\pi\pi}(s,t)$ at order p^2 which is given by

$$|T_{\pi\pi}(s,t)|^2=\frac{1}{F_\pi^4}[2(s^2+t^2+u^2)-9M_\pi^4]\ . \tag{5.19}$$

Equation (5.17) for the damping rate is exact to the order we are considering here. Note that here only the elastic $\pi\pi$ scattering amplitude enters. In the unitarity relation (5.9) S-matrix elements with more than two particles in the initial or final state only show up at the next order of the chiral perturbation series. The result in Eq. (5.17) has already been found in Ref. [3] where the decay of the probability distribution towards thermal equilibrium is analyzed using the master equation of kinetic theory.

Neglecting effects of Bose correlation in the initial and final states one can rewrite Eq. (5.17) in terms of the total cross section as

$$\gamma(p)=\frac{1}{\omega_p}\int\frac{d^3q}{(2\pi)^3 2\omega_q}n_B(\omega_q)\sqrt{s(s-4M_\pi^2)}\sigma_{\pi\pi}(s)\ . \tag{5.20}$$

The right-hand side indeed represents the collision rate for pions of momentum p traversing a pionic target whose momenta are distributed according to the Bose factor $n_B(\omega)$.

VI. COMMENTS

Before entering the numerical analysis, we add a few comments concerning the analytic structure of our result.

We first note that the Bose factor entering the first integral of Eq. (5.15) is to be evaluated at ω_p^T. At the one-loop level the interaction with the heat bath modifies the mass of the particles. Thus, the gas can actually be considered as a medium consisting of quasiparticles with an effective mass $M_\pi(T)$. The two-loop contribution in Eq. (4.25), depending on the tree result for the two-particle scattering amplitude,

$$T_{\pi\pi}^{\text{tree}}=-\frac{M_0^2}{F_0^2}\ , \tag{6.1}$$

indeed accounts for one part of this effect. It represents the correction to the contribution in Eq. (5.6), which occurs if the thermal distribution of the quasiparticles is evaluated with their effective mass $M_\pi(T)$. We could also replace the Bose factors in the second integral of Eq. (5.15) since this modification is beyond the accuracy of our representation. Yet, all momenta in the S-matrix elements of interest are still on the mass shell, defined by the mass M_π at zero temperature. Beyond the two-loop level, however, Eq. (4.25) will involve the then momentum-dependent two-particle amplitude beyond tree level and the temperature insertion (2.11) will drive the momentum q off its mass shell to the value $q^2=M_\pi^2(T)$. Thus, we are quite naturally led to consider off-shell extensions of S-matrix elements.

The off-shell extrapolation of the amplitude $A(s,t,u)$ is strongly constrained by Bose statistics and crossing symmetry. At order p^2 the most general form has only one free parameter and is given by

$$A(s,t,u)=\frac{1}{F_0^2}\left[s-M_0^2+\frac{\alpha}{5}\sum_i(p_i^2-M_0^2)\right]\ . \tag{6.2}$$

From Eq. (5.2) one readily obtains the following behavior for the $\pi\pi$ forward-scattering amplitude at leading order:

$$T_{\pi\pi}(p,q)=\frac{1}{F_0^2}[-M_0^2+2(\alpha+1)(p^2-M_0^2)$$
$$+2(\alpha+1)(q^2-M_0^2)]\ . \tag{6.3}$$

Allowing the momenta q in the two-particle S-matrix elements of definition (5.8) to be off shell does change the result for the proper three-particle amplitude as well. As previously discussed, the singular terms in the forward

limit of the three-particle scattering amplitude describe double forward-scattering events. These processes fall into two different classes. In the first case a probing particle with momentum p successively scatters with two particles of the heat bath. In the other case, this particle interacts with only one particle of the heat bath, which in turn interacts with a second particle of the medium. If one allows the momentum q in Eq. (5.8) to be off shell only in contributions of the first kind, one obtains the following forward limit for the newly defined proper amplitude $\tilde{T}_{\pi\pi\pi}$ at the tree level:

$$\tilde{T}_{\pi\pi\pi}=\hat{T}_{\pi\pi\pi}-4(\alpha+1)\frac{M_0^2}{F_0^2}\ . \tag{6.4}$$

Thus, a slight modification of the proper three-particle amplitude allows the self-energy to be rewritten in the form

$$\Sigma_R^T(\omega_p,\mathbf{p})=-\int\frac{d^3p}{(2\pi)^3 2\omega_q^T}n_B(\omega_q^T)T_{\pi\pi}(q^2=M_\pi^2(T),p^2=M_\pi^2)$$
$$-\frac{1}{2}\int\frac{d^3q_1}{(2\pi)^3 2\omega_{q_1}}\frac{d^3q_2}{(2\pi)^3 2\omega_{q_2}}n_B(\omega_{q_1})n_B(\omega_{q_2})\tilde{T}^{R}_{\pi\pi\pi}(p,q_1,q_2)\ . \tag{6.5}$$

First, one should note that the asymmetry between the momenta p and q in this result was put in by hand right from the beginning since the self-energy in Eq. (4.20) was approximated by its value at the position $\omega_p^2=\mathbf{p}^2+M_\pi^2$. A more symmetric result can probably be obtained by allowing all momenta in definition (5.8) to be off shell and by using a better approximation for the self-energy.

Including off-shell extensions of two-particle amplitudes amounts to shifting some contributions from the second term in Eq. (5.15) to the first one without changing the final result for the pole position. To some extent both, two- and three-particle S-matrix elements describe contributions generated by two successive two-particle scattering events of the propagating particle in the medium. Because of the lack of asymptotic states in the heat bath there is no clear-cut distinction between the two. Furthermore, corrections of second order in the density can by no means be estimated by neglecting the three-particle processes but including an arbitrary off-shell extension of the two-particle amplitude.

The scattering amplitudes entering Eq. (5.15) refer to zero temperature. Since temperature drives the pole position away from $p^2=M_\pi^2$, one may wonder whether the result could not be written in a more transparent manner by expressing it in terms of a scattering amplitude at finite temperature describing the scattering of particles in a heat bath. A straightforward generalization of the amplitude $A(s,t,u)$ to nonzero temperature would be a definition of the form

$$i^3\int dz_1dz_2dz_3\exp(ip_1z_1+ip_2z_2+ip_3z_3+ip_4z_4)\langle R[A_0^{k_1}(z_1)A_0^{k_2}(z_2)A_0^{k_3}(z_3)A_0^{k_4}(z_4)]\rangle$$
$$\doteq p_1^0p_2^0p_3^0p_4^0\frac{F_\pi^4(T)}{\prod(p_i^2-M_\pi^2(T))}(\delta^{k_1k_2}\delta^{k_3k_4}A^{R,T}(p_1,p_2;p_3,p_4)+\cdots)\ , \tag{6.6}$$

which purposely involves the retarded product. A one-loop calculation will show that the corresponding function for the time-ordered product does not have a well-defined forward limit. Thus, Feynman boundary conditions are not appropriate for the description of scattering processes in the heat bath, which should not come as a big surprise and should be related to the nonexistence of asymptotic states in the medium. Furthermore, the retarded structure does show up in the temperature-dependent corrections only: in the limit of vanishing temperature we recover the amplitude $A(s,t,u)$.

Since some of the temperature-dependent corrections can be written as an integral over the Bose factor and the retarded proper three-particle amplitude one could expect the following result for the self-energy in terms of the temperature-dependent amplitude:

$$\Sigma_R^T=-\int\frac{d^3q}{(2\pi)^3 2\omega_q^T}n_B(\omega_q^T)T^{R,T}_{\pi\pi}\ . \tag{6.7}$$

Unfortunately, this is not the case. An explicit calculation shows that all contributions of second order in the density are too large by a factor of 2. This result resembles the final-state interaction theorem which also involves the factor $e^{i\delta}$ rather than the full S-matrix element $e^{2i\delta}$. Intuitively, the factor of 2 can be understood as follows. In the scattering problem, the interaction is at work from $t=-\infty$ to $+\infty$, i.e., both when the particles approach one another and when they recede. The propagator, on the other hand, describes the evolution of a disturbance inserted into the medium at $t=0$. Here, the interaction is operative only from $t=0$ to $+\infty$.

VII. NUMERICAL RESULTS

The results of our chiral perturbation theory calculation to two loops can unambiguously be expressed in terms of M_π, F_π and two scattering length parameters: the combination $a_0^0+5a_0^2$ of $I=0$ and 2 s waves and a_2^0 of

the $I=0$ d wave. Chiral perturbation theory predicts [14]

$$a_0^0=0.20\pm0.01\ ,\quad a_0^2=-0.042\pm0.002\ . \tag{7.1}$$

The combination $a_0^0+5a_0^2$ is therefore very small. For the d wave, we use the experimental value of Petersen [15]:

$$a_2^0=(17\pm3)\times10^{-4}M_\pi^{-4}\ . \tag{7.2}$$

With this input, we have a parameter-free prediction which specifies the dispersion law $\omega(p)$ as well as the absorption rate $\gamma(p)$ as a function of temperature and momentum which accounts for all contributions up to and including $O(p^5)$.[1] Note that the calculation accounts both for contributions proportional to the density of the gas (two-particle collisions) as well as for terms of order n_B^2 (three-particle collisions). The other side of the coin is that the first two terms in the chiral expansion provide an adequate representation of the relevant scattering amplitudes only at small momenta so that our result is reliable only for low temperatures and long wavelengths. To illustrate the problem, we consider the real part of the elastic forward-scattering amplitude. The relevant isospin combination

$$T_{\pi\pi}(s)=\frac{1}{3}[T^0(s)+3T^1(s)+5T^2(s)] \tag{7.3}$$

is shown in Fig. 4.

The dashed line is the chiral perturbation theory representation to one loop, given explicitly in Eq. (5.5). The two dashed-dotted lines represent unitarized versions of this result and will be discussed below. The shaded area represents the result of a semiphenomenological analysis [6] of the relevant scattering amplitude, using chiral perturbation theory at threshold and relying on experimental information at higher energies. The width reflects the uncertainty of the experimental input. This analysis accounts for effects generated by ρ exchange and yields a reliable prediction for the scattering amplitude in regions where an expansion in powers of momenta is no longer useful. By comparison we can estimate the range of validity of the chiral representation. Note that at $T=100$ MeV, the mean pion energy is of order 300 MeV; accordingly, collisions with $\sqrt{s}\simeq600$ MeV will occur rather frequently at this temperature. Figure 4 shows that current algebra [lowest order chiral perturbation theory (χPT), dotted horizontal line] does not adequately represent the scattering amplitude at these energies. The failure of the current algebra prediction is due to the fact that, in the isospin averaged forward amplitude, the s- and p-wave contributions nearly cancel. In the chiral limit, $T_{\pi\pi}$ contains an Adler zero at $s=0$ and the corresponding tree-level amplitude vanishes altogether. Our calculation shows indeed, that corrections of order p^4 to this amplitude lead to substantial modifications. The result (dashed line) represents a decent approximation of the scattering amplitude up to $\sqrt{s}\lesssim700$ MeV at the 20% level. Above this energy, the chiral representation overshoots, because it violates unitarity.

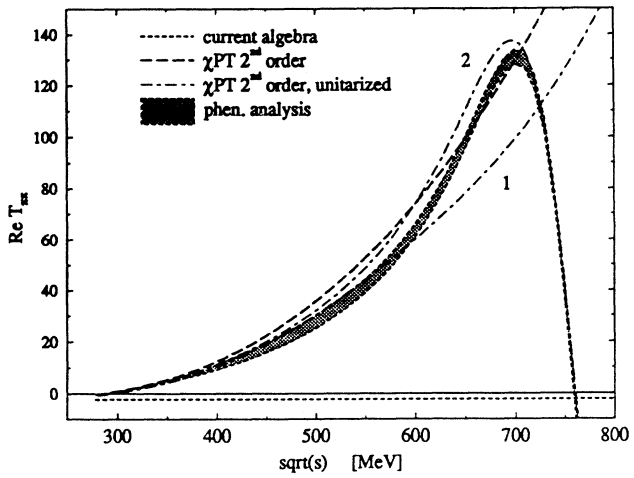

FIG. 4. Real part of the isospin averaged $\pi\pi$ forward-scattering amplitude.

The violation of unitarity originates in the truncation of the chiral perturbation series at order p^4. It is not difficult to remedy this deficiency in the elastic region $4M_\pi^2\le s\le16M_\pi^2$. There unitarity implies that the partial-wave amplitudes $T_l^I(s)$ are determined by the phase shifts $\delta_l^I(s)$ according to

$$T_l^I(s)=\left[\frac{s}{s-4M_\pi^2}\right]^{1/2}e^{i\delta_l^I}\sin\delta_l^I\ . \tag{7.4}$$

To unitarize the chiral representation, it thus suffices to express the scattering amplitude in terms of the partial waves, using chiral perturbation theory for the phase shifts rather than for the amplitude itself. The procedure ensures that the resulting representation for the scattering amplitude does not terminate at $O(p^4)$, but contains higher-order contributions as required by unitarity. The problem is that the procedure does not fix these higher-order terms uniquely, because a one-loop calculation of the scattering amplitude only determines the phase shifts to accuracy p^4. We illustrate the ambiguity inherent in the unitarization procedure by giving two specific examples.

Consider first the systematic expansion of the phase shifts in powers of the momentum, which is determined by the real part of the partial waves [16]:

$$\delta_l^I(s)=\left[\frac{s-4M_\pi^2}{s}\right]^{1/2}\mathrm{Re}T_l^I(s)+O(p^6)\ . \tag{7.5}$$

Although this formula is not exact, the difference is of order $(\delta_l^I)^3=O(p^6)$ and therefore beyond the accuracy of the one-loop representation.

The effective range approximation for the cotangent of the phase shift suggests an alternative unitarization prescription [17]. The contangent is related to the real part of the inverse scattering amplitude:

[1]Recall that in this bookkeeping $|\mathbf{p}|$, T, and M_π count as quantities of order p.

$$\mathrm{Re}\left[\frac{1}{T_l^I(s)}\right]=\left[\frac{s-4M_\pi^2}{s}\right]^{1/2}\cot\delta_l^I\ . \tag{7.6}$$

In the elastic region, this relation is exact. Truncating the chiral series for the left-hand side at a given order, the formula can be solved for δ_l^I, thus providing us with a second representation of the scattering amplitude which also obeys elastic unitarity and is correct to order p^4 in the chiral expansion.

Algebraically, the difference between the two unitarization prescriptions (7.5) and (7.6) is the following. The tree graph contribution to the scattering amplitude is real and is of order $\mathcal{O}(p^2)$. In particular,

$$T^0_{0,\mathrm{tree}}=\frac{2s-M_\pi^2}{32\pi F_\pi^2}\ , \tag{7.7}$$

$$T^2_{0,\mathrm{tree}}=\frac{2M_\pi^2-s}{32\pi F_\pi^2}\ , \tag{7.8}$$

$$T^1_{1,\mathrm{tree}}=\frac{s-4M_\pi^2}{96\pi F_\pi^2}\ . \tag{7.9}$$

Writing the chiral expansion for $\mathrm{Re}T_l^I$ in the form

$$\mathrm{Re}T_l^I=T^I_{l,\mathrm{tree}}[1+\epsilon_l^I+O(p^4)] \tag{7.10}$$

the prescriptions (7.5) and (7.6) amount to

$$\left.\begin{matrix}\delta_l^I\\ \tan\delta_l^I\end{matrix}\right\}=\left[\frac{s-4M_\pi^2}{s}\right]^{1/2}T^I_{l,\mathrm{tree}}\times\begin{cases}(1+\epsilon_l^I) & (7.5')\\ (1-\epsilon_l^I)^{-1}\ . & (7.6')\end{cases}$$

Either of the two correctly reproduces the chiral expansion of the scattering amplitude up to and including terms of order p^4.

Figure 5 illustrates the situation for the p wave. The full line represents the result of the semi-phenomenological analysis [6]. The dashed and dashed-dotted lines are based on the evaluation of Eqs. (7.5') and (7.6'), respectively. This evaluation involves the following steps. In the form given in Eq. (5.3), the chiral perturbation theory representation of the scattering amplitude contains the effective coupling constants F_0, $\bar{L}_1$, and $\bar{L}_2$. In the corresponding representation for the partial-wave amplitude $\mathrm{Re}T_1^1$, we have eliminated these constants in favor of the threshold parameters a_1^1 and b_1^1. Chiral symmetry predicts the following values for these quantities [14]:

$$a_1^1=0.038\pm0.002\ ,\quad b_1^1=(5\pm3)\times10^{-3}\ . \tag{7.11}$$

The quantity $1+\epsilon_1^1$ is given by the ratio $\mathrm{Re}T_1^1/T^1_{1,\mathrm{tree}}$. As indicated in Eq. (7.7), we are evaluating the tree amplitude which occurs in the unitarization prescription with the physical values of F_π, M_π.

Unfortunately, the χPT prediction for b_1^1 is subject to a large uncertainty. The unitarization (7.6') does imply the occurrence of a resonance, but its mass varies from 550 to 920 MeV if b_1^1 is varied in the range given in Eq. (7.11). The dash-dotted line shown in the figure results if one

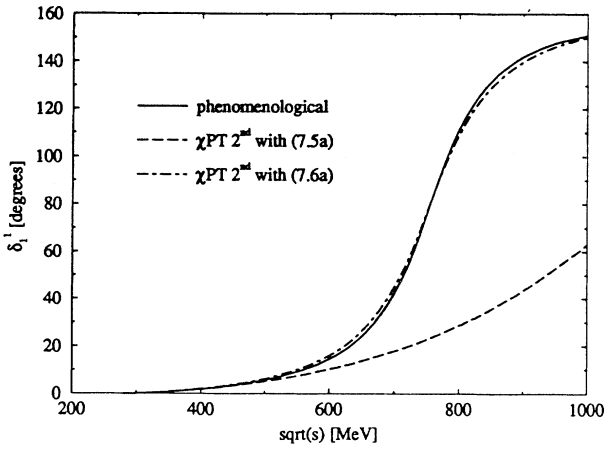

FIG. 5. p-wave phase shift of the $\pi\pi$ scattering amplitude.

fixes the effective range in such a way that the resonance occurs at the physical mass $M_\rho=769$ MeV; this requires $b_1^1=3.5\times10^{-3}$. Figure 5 shows that this particular unitarization of the chiral one-loop calculation essentially coincides with the result of the phenomenological analysis. The small difference in the slope at the resonance is due to the fact that the full line also correctly reproduces the experimental value of the ρ width, $\Gamma_\rho=149$ MeV, which is accounted for by another parameter in the phenomenological analysis. Note, that Eq. (7.5'), on the other hand, predicts a phase shift that passes through 90° well above $\sqrt{s}=1$ GeV. (In the figure, we have evaluated this equation with the central value $b_1^1=5\times10^{-3}$.) Below the $K\bar{K}$ threshold, partial waves with $l\geq2$ generate negligibly small contributions. Dropping these, the isospin-averaged forward-scattering amplitude becomes

$$T_{\pi\pi}=\frac{32\pi}{3}(T_0^0+9T_1^1+5T_0^2)\ . \tag{7.12}$$

Evaluating the partial waves with the prescription (7.5') one arrives at curve 1 in Fig. 4, while the prescription (7.6') leads to curve 2. The range between these two curves indicates the ambiguity inherent in the unitarization procedure. The s wave violates unitarity already at rather low energies, which is mainly responsible for the difference between the chiral approximation (5.5) for the scattering amplitude and the two unitarized chiral representations in the region $\sqrt{s}\approx500$ MeV.

The numerical result for the temperature dependence of the effective mass $M_\pi(T)$ is shown in Fig. 6. The full line describes the result of our calculation, as given in expression (5.15). It includes effects of first and second order in the density. The main point to notice is the smallness of the mass shift: For $T=100$ MeV the mass is lowered by an amount of merely 2.5% while at $T=150$ MeV it is reduced by 14%. The remaining lines in this figure are determined by the numerical evaluation of expression (5.6), which includes only effects of first order in

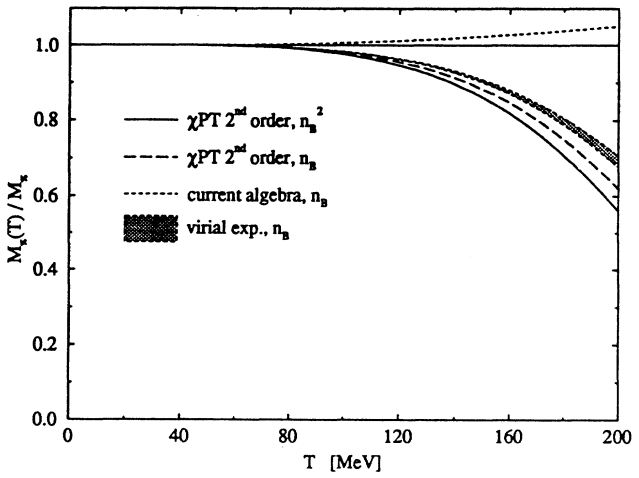

FIG. 6. Pion mass as a function of temperature. Results of first order in the density are obtained by evaluating expression (5.6) with various approximations for the $\pi\pi$ forward-scattering amplitude. The full result, including all corrections of second order in the density is obtained by evaluating expression (5.15).

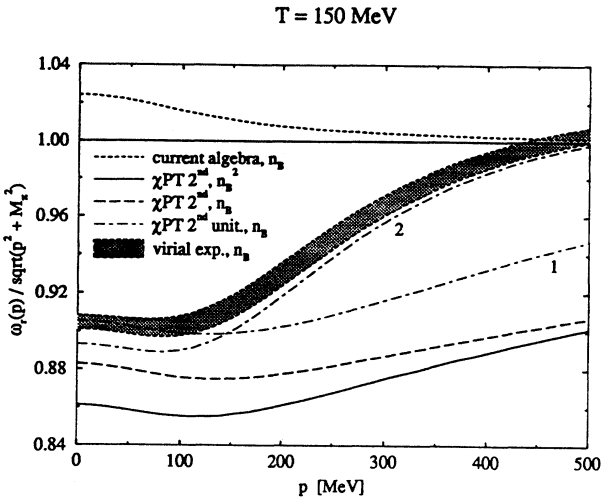

FIG. 7. Pion energy $\omega(p)$ divided by the free particle energy ω_p. Temperature is $T=150$ MeV. Results of first order in the density are obtained by evaluating expression (5.6) with various approximations for the $\pi\pi$ forward-scattering amplitude. The full result, including all corrections of second order in the density is obtained by evaluating expression (5.15).

the density, and are based on the various approximations for the $\pi\pi$ scattering amplitude introduced above. To discuss the importance of the higher-order terms which our calculation neglects, we make the following observations.

(1) Effects of order n_B^2, given by the difference between the full line and the dashed line [see (2) below], turn out to be very small: even at $T=150$ MeV they lower the effective mass by only 2.5%, arising mainly from three-body collisions (the effects of the mass shift in the Bose factor are of order 0.2%). Figure 7 shows that this result also holds for the dispersion $\omega(p)$ at nonzero momenta. This indicates that the main contribution stems from the terms of first order in the density, i.e., the first term in the virial expansion.

(2) Equation (4.22) together with expression (5.6) for the self-energy represents an exact formula for the first term in the virial expansion. It expresses the dispersion law in terms of the real part of the isospin averaged forward-scattering amplitude. The shaded area in Fig. 6 is the result for the phenomenological analysis of the forward amplitude while the dashed line is evaluated with the chiral representation (5.5) for $\mathrm{Re}T_{\pi\pi}$. As was to be expected, the chiral representation overestimates the effect, but still provides an adequate description for $T \lesssim 150$ MeV. Note that the current algebra curve (dotted line) is entirely fictitious already at very low values of T.

(3) The result for $\omega(p)$, displayed in Fig. 7, confirms that temperature effects are small: The dispersion law of pions traveling in a medium closely resembles the one in vacuo: even for $T=150$ MeV, the scattering with the gas modifies the frequency by less than 20%. In particular, in the low-temperature long-wavelength region analyzed here, we do not find any indication for qualitative changes in the dispersion law such as those envisaged in Ref. [18].

(4) The curve for $\omega(p)$ also illustrates the inadequacies of the chiral expansion for the scattering amplitude $T_{\pi\pi}$ to order p^4 (compare the dashed line with the shaded area). For long wavelength ($p \lesssim 150$ MeV), the region 400 MeV $\lesssim \sqrt{s} \lesssim 600$ MeV again leads to an overestimate of the temperature effects but the approximation is not bad. As p grows the region around the ρ resonance becomes more important and the straightforward chiral representation then goes astray. The importance of higher-order contributions is nicely shown by the two dashed-dotted lines in Fig. 7, which correspond to the two unitarized chiral representations above.

Note, that our analysis of the dispersion law at order n_B^2 involves the numerical evaluation of the principal-value integral in Eq. (5.15). To ensure correctness we have carefully checked our numerical results using various different methods of integration.

Figure 8 shows the result for the mean damping rate,

$$\bar{\gamma}^T = \langle \gamma(p) \rangle = \int d^3p\, n_B(\omega_p)\gamma(p) \Big/ \int d^3p\, n_B(\omega_p)\,, \tag{7.13}$$

as a function of temperature. The full line describes the result of our calculation, given explicitly in Eq. (5.17). Neglecting Bose correlation in the initial and final states, the remaining lines in this figure are determined by the numerical evaluation of expression (5.20) and are based on various approximations for the total $\pi\pi$ cross section. To compare the results for the mean damping and for the dispersion law, we observe the following.

(1) Effects from Bose correlation, given by the difference between the dotted line [see (2) below] and the full one, are very small: they increase the mean damping

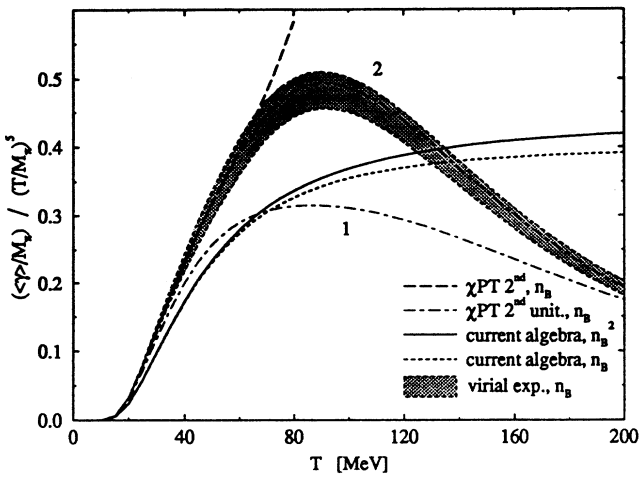

FIG. 8. The mean damping rate divided by the fifth power of temperature. Results of first order in the density are obtained by evaluating expression (5.20) with various approximations for the total $\pi\pi$ cross section. The full result, including all corrections of second order in the density is obtained by evaluating expression (5.17).

by an amount of less than 6%. This indicates that the main contribution to the damping rate again stems from terms of first order in the density.

(2) Equation (5.20) represents an exact formula for the first term of the virial expansion, expressing the damping rate in terms of the isospin averaged total $\pi\pi$ cross section. Since the total cross section is determined by the forward-scattering amplitude through the optical theorem, Eq. (4.24) together with expression (5.6) provides an equivalent representation for this formula. Again the shaded area in Fig. 8 is the result of the phenomenological analysis for the forward-scattering amplitude, while the dotted line is evaluated with the current algebra representation for the total cross section:

$$\sigma_{\pi\pi}=\frac{5}{48\pi F_\pi^4}s\left[1-\frac{4}{5}\left[\frac{4M_\pi^2}{s}\right]+\frac{37}{160}\left[\frac{4M_\pi^2}{s}\right]^2\right] . \tag{7.14}$$

Since the imaginary parts of the partial-wave amplitudes obey the positivity condition

$$\mathrm{Im}T_l^I\geq 0 , \tag{7.15}$$

cancellations cannot occur. Thus, in the case of the total cross section the current algebra representation should provide a better approximation to the phenomenological parametrization than was to be observed for the real part of the scattering amplitude. This is indeed born out in Fig. 8, which shows that the corresponding predictions for the mean damping agree within 30% at temperatures below 100 MeV.

(3) We recall, that at a temperature of 100 MeV both collision partners in Eq. (7.13) have energies of about 300 MeV. Thus, in the range $T\gtrsim 100$ MeV predictions for the mean damping which are based on chiral representations for the cross section have to be considered with care. This is indeed confirmed by the dashed line in Fig. 8, which is evaluated with Eq. (5.20) and the chiral representation for the total cross section at order p^4. At this order, the cross section is determined by the amplitude $A(s,t,u)$, given in Eq. (5.3). Note, that the $I=0$ s wave at order p^4 strongly violates the unitarity bound at energies $\sqrt{s}\gtrsim 600$ MeV, which explains the imminent growth of this approximation with temperature. The dashed-dotted line marked 2 (lying in the shaded area) is based on the unitarization prescription (7.6′) and shows a decent behavior over the whole range of temperatures. Line 1, on the other hand, is based on prescription (7.5′) and indicates the importance of ρ exchange to the damping of pionic waves already at rather low temperatures (compare also with Fig. 5).

(4) The phenomenological analysis predicts the quantity $\bar{\gamma}/T^5$ to decrease by more than a factor of 2 at temperatures between 90 and 200 MeV. This result, however, only accounts for the damping in a medium that consists exclusively of pions. As the temperature rises, the heat bath also contains a significant number of other particles, such as $K,\rho,\eta,\ldots$, which increase the damping rate. Including these effects, the mean damping of pions was found [13] to behave approximately like $T^5/12F_\pi^4$ at temperatures above 100 MeV.

VIII. SUMMARY AND CONCLUSIONS

The propagation properties of pions in hot matter are governed by the position of the pole occurring in the various Green's functions, e.g., the retarded two-point function of the axial-vector current. For real values of the three-momentum $p=|\mathbf{p}|$, the pole sits at a complex value of the energy:

$$p^0=\omega(p)-(i/2)\gamma(p) . \tag{8.1}$$

The real part $\omega(p)$ describes the dispersion of pionic waves while the absorptive properties are determined by the imaginary part $\gamma(p)$. At infinite wavelength $p=0$, the pole occurs on the real axis; its position depends on the temperature and is referred to as the effective mass

$$M_\pi(T)=\omega(0) . \tag{8.2}$$

At low temperatures, the gas is dilute and it is therefore appropriate to use the virial expansion where the various quantities of interest are represented as a power series in the particle density. The leading term in the virial expansion of the damping rate is proportional to the density:

$$\gamma(p)=\frac{1}{\omega_p}\int\frac{d^3q}{(2\pi)^3 2\omega_q}n_B(\omega_q)\sqrt{s(s-4M_\pi^2)}\sigma_{\pi\pi}(s) , \tag{8.3}$$

where $\sigma_{\pi\pi}$ is the isospin averaged total $\pi\pi$ cross section. At the same order in the density, the dispersion law is given by

$$\omega(p)=\omega_p-\frac{1}{2\omega_p}\int\frac{d^3q}{(2\pi)^3 2\omega_q}n_B(\omega_q)\mathrm{Re}T_{\pi\pi}(s) , \tag{8.4}$$

where $T_{\pi\pi}$ is the isospin averaged $\pi\pi$ forward-scattering amplitude. Both expressions can be evaluated with phenomenological parameterizations of the cross section and the forward-scattering amplitude which are based on experimental data on $\pi\pi$ scattering. Comparing these results with the corresponding prediction of chiral perturbation theory, one can estimate the range of validity of the chiral expansion and analyze the importance of ρ exchange for the propagation properties.

In the chiral expansion, the leading corrections to the pole shift are determined by the tree-level amplitude $T_{\pi\pi}=-M_\pi^2/F_\pi^2$. They are independent of the momentum and merely renormalize the pion mass, which becomes a function of temperature. In accordance with unitarity, absorption and dispersion only show up if next-to-leading-order corrections are included. After isospin averaging, the s- and p-wave contributions to the $\pi\pi$ forward-scattering amplitude cancel to a large extent, which explains why current algebra (chiral perturbation theory at leading order) fails even qualitatively, predicting an effective mass that increases with temperature.

Corrections of next-to-leading order in the low-temperature expansion include effects of first and second order in the density.

At first order in the density the pole shift is now determined by the one-loop result for the $\pi\pi$ forward-scattering amplitude. As expected, we indeed get large corrections to the leading-order prediction of chiral perturbation theory; in particular the effective mass $M_\pi(T)$ now decreases with temperature. The comparison of this result for the pole shift with an earlier analysis based on a phenomenological description of the $\pi\pi$ scattering amplitude shows that both predictions for the effective mass and for the quasiparticle energy $\omega(p)$ agree within 20% at temperatures and momenta below 150 MeV. At higher momenta the effect of ρ exchange clearly shows up. At leading order, the damping rate is determined by the current algebra result for the total $\pi\pi$ cross section, or equivalently, by the imaginary part of the $\pi\pi$ forward-scattering amplitude at order p^4. At temperatures below 100 MeV, this prediction for the mean damping agrees with the result based on the phenomenological analysis to within 30% which is much better than what has been observed for the dispersion law. Because of the positivity condition $\mathrm{Im}T_l^I \geq 0$, cancellations between different partial waves cannot occur here and a better agreement for the damping was indeed to be expected. If the total $\pi\pi$ cross section is evaluated at order p^4 (next-to-leading order), we observe a decent agreement between the semi-phenomenological analysis of the mean damping rate and the prediction of chiral perturbation theory at temperatures below 80 MeV. At a temperature of 100 MeV, the energy of both collision partners is of order 300 MeV and the chiral prediction in this range of temperatures is no longer reliable. As the temperature rises, the heat bath furthermore contains a significant number of other excitations, such as $K,\rho,\eta,\ldots$, which increase the damping. Including these effects, the mean damping of pions was found [13] to behave approximately like $T^5/12F_\pi^4$ at temperatures above 100 MeV.

The next term in the virial expansion is a much more complicated matter. We have shown that both the absorptive and dispersive properties are determined by the forward limit of two- and three-particle scattering amplitudes. The latter contain successive two-particle scattering events which generate singularities in the forward direction. Removing these singularities, we have introduced a proper three-particle scattering amplitude and we have shown that the pole shift can be expressed in terms of this object. Although the definition of the proper amplitude involves an off-shell extrapolation which is not unique, the result for the pole shift is independent of the particular extrapolation used. The occurrence of off-shell contributions is related to the fact that the asymptotic states occurring in the definition of the S matrix are not relevant if the pions are moving through a medium. We have explored the possibility of defining an effective scattering matrix describing collisions in this medium. The corresponding two-particle amplitude indeed contains contributions from three-body collisions. Replacing the zero-temperature quantity $\mathrm{Re}T_{\pi\pi}$ in Eq. (8.4) by this effective thermal scattering amplitude, and replacing the pion mass by the effective thermal mass, one indeed arrives at an expression for the pole shift which resembles the correct result. The prescription, however, counts the terms of second order in the particle density twice and can therefore not be used as a substitute for the actual calculation. Numerically, the second order terms are quite small. Evaluating these contributions with chiral perturbation theory, we find that they lower the effective mass and the damping rate by 2.5% and 6%, respectively.

Thus, the main results of our numerical analysis can be summarized by the following two observations: (1) Effects of order n_B^2 are very small. The main contribution to both, the dispersion law and the damping stem from the first term in the virial expansion. (2) Temperature effects on the energy and the mass are small. The dispersion law of pions traveling in hot matter closely resembles the one *in vacuo*. In particular, we do not find any qualitative changes in the dispersion law such as those envisaged in Ref. [18].

ACKNOWLEDGMENTS

It is a pleasure to thank Professor H. Leutwyler for many enlightening discussions and his encouragement during several steps of this work as well as for his critical reading of this manuscript. This work was supported in part by Schweizerischer Nationalfonds and by Studienstiftung des Deutschen Volkes.

[1] *Quark Matter '88,* Proceedings of the Seventh International Conference on Ultrarelativistic Nucleus-Nucleus Collisions, Lenox, Massachusetts, 1988, edited by G. Baym, P. Braun-Munzinger, and S. Nagamiya [Nucl. Phys. **A498**, 1 (1989)]; *Quark Matter '90,* Proceedings of the Eighth International Conference on Ultrarelativistic Nucleus-Nucleus Collisions, Menton, France, 1990, edited by J. Blaizot *et al.* [Nucl. Phys. **A525**, 1 (1991)]; *Quark Matter*

'91, Proceedings of the Ninth International Conference on Ultrarelativistic Nucleus-Nucleus Collisions, Gatlinburg, Tennessee, 1991, edited by T. C. Awes *et al.* [Nucl. Phys. **A544**, 1 (1992)].
[2] P. Gerber and H. Leutwyler, Nucl. Phys. **B321**, 387 (1989).
[3] J. Goity and H. Leutwyler, Phys. Lett. B **228**, 517 (1989).
[4] J. Gasser and H. Leutwyler, Phys. Lett. B **184**, 83 (1987).
[5] H. Leutwyler and A. V. Smilga, Nucl. Phys. **B342**, 302 (1990).
[6] A. Schenk, Nucl. Phys. **B363**, 97 (1991).
[7] E. V. Shuryak, Nucl. Phys. **A533**, 761 (1991).
[8] N. P. Landsman and Ch. G. van Weert, Phys. Rep. **145**, 141 (1987). This review contains a comprehensive list of references to the original literature of field theory at finite temperature.
[9] H. Leutwyler, in *Proceedings of the Workshop on Effective Field Theories of the Standard Model,* Dobogókö, Hungary, 1991, edited by Ulf-G. Meissner (World Scientific, Singapore, 1992).
[10] J. Gasser and H. Leutwyler, Ann. Phys. (N.Y.) **158**, 142 (1984).
[11] R. J. Eden, P. V. Landshoff, D. I. Olive, and J. C. Polkinghorne, *The Analytic S-Matrix* (Cambridge University Press, Cambridge, England, 1966).
[12] D. Iagolnitzer, J. Math. Phys. **6**, 1576 (1965); K. Hepp, *ibid.* **6**, 1762 (1965); G. Wanders, Helv. Phys. Acta **38**, 142 (1965).
[13] H. Bebie, P. Gerber, J. L. Goity, and H. Leutwyler, Nucl. Phys. **B378**, 95 (1992).
[14] J. Gasser and H. Leutwyler, Phys. Lett. **125B**, 325 (1983).
[15] J. L. Petersen, CERN Yellow Report, 77-04, 1977 (unpublished).
[16] J. Gasser and Ulf-G. Meissner, Phys. Lett. B **258**, 219 (1991).
[17] D. Dobado, M. J. Herrero, and T. N. Truong, Phys. Lett. B **235**, 134 (1990).
[18] E. V. Shuryak, Phys. Rev. D **42**, 1764 (1990).